Conception and Evaluation of Fluorescent Phosphine-Gold Complexes: From Synthesis to in vivo Investigations

Benjamin Rousselle, Aurélie Massot, Malorie Privat, Lucile Dondaine, Audrey Trommenschlager, Florence Bouyer, Jérôme Bayardon, François Ghiringhelli, Ali Bettaieb, Christine Goze, et al.

Conception and evaluation of fluorescent phosphine-gold complexes: from synthesis to *in vivo* investigations

Dr. Benjamin Rousselle,[a] Aurélie Massot,[b] Dr. Malorie Privat,[a,b] Lucile Dondaine,[a,b] Dr. Audrey Trommenschlager,[a] Dr. Florence Bouyer,[c] Dr. Jérôme Bayardon,[a] Prof. François Ghiringhelli,[c] Prof. Ali Bettaieb,[b] Dr. Christine Goze,[a] Prof. Catherine Paul,[b]* Dr. Raluca Malacea-Kabbara,[a]* and Prof. Ewen Bodio[a]*

[a] B. Rousselle, M. Privat, L. Dondaine, A. Trommenschlager, J. Bayardon, C. Goze, R. Malacea-Kabbara,* and E. Bodio*
ICMUB, UMR CNRS 6302,
University Bourgogne Franche-Comté,
Dijon 21000 Dijon, France
E-mail: Raluca.Malacea@u-bourgogne.fr, Ewen.Bodio@u-bourgogne.fr

[b] A. Massot, M. Privat, L. Dondaine, A. Bettaieb, C. Paul,*
Laboratoire d'Immunologie et Immunothérapie des Cancers,
EPHE, PSL Research University, Université de Bourgogne,
Dijon 21000, France
Email: catherine.paul@u-bourgogne.fr

[c] F. Bouyer, F. Ghiringhelli
INSERM UMR 1231,
Université Bourgogne Franche-Comté,
Dijon 21000, France

Supporting information for this article is given via a link at the end of the document

Abstract: A phosphine gold(I) and phosphine-phosphonium gold(I) complexes bearing a fluorescent coumarin moiety were synthesized and characterized. Both complexes displayed interesting photophysical properties: good molar absorption coefficient, good quantum yield of fluorescence, and ability to be tracked *in vitro* thanks to two-photon imaging. Their *in vitro* and *in vivo* biological properties were evaluated onto cancer cell lines both human and murine and into CT26 Tumor-bearing BALB/c mice. They displayed moderate to strong antiproliferative properties and the phosphine-phosphonium gold(I) complex induced significant *in vivo* anti-cancer effect.

Introduction

The research of new antineoplastic agents has been giving pride of place to metal-based drugs for years and more particularly since the discovery of the anticancer properties of cisplatin by Rosenberg.[1,2] While many researches have focused on platinum derivatives,[3–5] the anti-cancer properties of many other metals such as titanium,[6] ruthenium[7]... have been investigated.[8–20]
In our case, we are interested in gold salts.[21–24] They have been used since ancient times and are still under investigation today. Indeed, gold complexes have been exploited in modern medicine to fight against parasitic and bacterial infection, or inflammation phenomena.[25–28] Additionally, the structural analogy of certain gold (III) complexes with cisplatin has inspired some researchers to investigate their potential in fighting cancer.[29–32] Various studies have opened up new avenues by stabilizing these complexes and showing that in a biological environment, they could be reduced to gold (I), which initiated research on gold (I) complexes.[31,33,34] However, it was the repositioning of auranofin, the drug used to treat acute rheumatoid arthritis, as an anti-cancer drug, that really kick-started the development of anti-cancer gold complexes.[35] Indeed, this phosphine-gold complex with a peracetylated thioglucose as "X" ligand is now being studied in several clinical trials for the treatment of different types of cancer (e.g. Epithelial Ovarian, Primary Peritoneal, Fallopian Tube Cancer [NCT01747798, NCT03456700], Chronic Lymphocytic Leukemia [NCT01419691], Non-Small Cell Lung Cancer [NCT01737502]…).[36–40]

Thus, for the past ten years, we have been developing various gold complexes with a preference for phosphine-gold derivative,[41–46] and, if possible, complexes, which can be tracked by optical imaging.[18,21,23,47–52] The development of such trackable therapeutics enabled us to get crucial information on the behavior of such new therapeutics *in vitro*. In particular, we developed a smart fluorescent "ON / OFF" probe.[49,53] It allowed us to prove that the P-Au bond was stable *in vitro* and *in vivo* (in zebrafish larvae), in contrast to commonly received ideas that this bond degrades in a biological environment. More precisely, the fluorescence of our system is quenched when the P-Au bond is broken (Figure 1, upper left part). Interestingly, this coumarin-based probe associated with gold (I) exhibited interesting antiproliferative properties on cancer cells, while not showing significant toxicity in zebrafish. The choice of coumarin as a fluorophore was not made at random. Indeed, this fluorophore is perfect for in vitro imaging: it is stable, has a good brightness and responds even in two-photon imaging. Moreover, it also presents interesting biological properties, either as an antibacterial or anti-inflammatory agent.[54–58] This last property is interesting because gold(I) complexes often also have anti-inflammatory properties. Knowing that some anti-cancer treatments induce inflammation phenomena which seem to be the cause of side effects,[59,60] the development of a drug with an anti-inflammatory effect should make it possible to limit such issues.

In addition, we have shown in a recent study that combining a phosphonium moiety with a phosphine-gold complex increases dramatically the anti-proliferative properties of the resulting molecule with regards to corresponding gold complex (Figure 1, upper right part).[61] Indeed, the phosphonium group allows to improve the crossing of cell membranes thanks to the combination of the water-solubilizing character of its positive charge and the lypophilicity due to the delocalization of this charge, when phosphonium is substituted by aromatic groups.[62] Moreover, phosphoniums are known to target mitochondria and have intrinsic anticancer activity.[63,64] In the present study (Figure 1, bottom part), we therefore decided to combine these two strategies in order to optimize the previous systems and to benefit from their respective advantages: *i.e.* to have a trackable gold complex (green part), which has a strong antiproliferative activity (orange part). Thus, in a first step, the target compound was synthesized, characterized and its photophysical, antiproliferative, and fluorescence properties *in vitro* were compared to those of previously reported compounds. In a second step, an *in vivo* study was performed to determine which is the most promising theranostic.

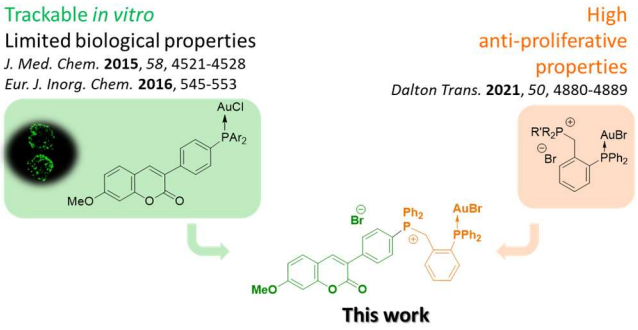

Figure 1. Illustration of the strategy developed in this work: combination of the work we have done on smart theranostics (coumarin-phosphine-gold complexes, green part)[49,53] and on phosphine-phosphonium-gold complexes (orange part)[61]

Results and Discussion

Synthesis

Obtaining phosphine-phosphonium complexes involves an alkylation reaction of a phosphine of interest with a (2-bromomethylphenyl)phosphine derivative. In our case, the phosphine of interest is the coumarin phosphine that we used previously to synthesize the smart theranostic. It is synthesized in two steps according to the strategy reported by Prat and coll (Scheme 1).[65] The first step consists in a cyclization reaction between 4-iodophenylacetonitrile and 2-hydroxy-4-methoxybenzaldehyde in presence of piperidine, which results in the coumarin core **III**. Then, an organometallic coupling enables the introduction of the chosen phosphine. On the other side, [(2-bromomethyl)phenyl] diphenylphosphine borane **IX** is obtained in three steps (Scheme 1):[61] reaction of 2-bromobenzyl alcohol with chlorodiphenyl phosphine and DIPEA, followed by boration with BH_3, then a halogen-metal exchange is carried out in the presence of *t*BuLi allowing a phospha-Fries rearrangement to give [(2-hydroxymethyl)phenyl] phosphine borane **VIII** (these different changes are easily monitored by ^{31}P-NMR), and the desired intermediate is finally obtained thanks to the Appel's reaction, which allows the conversion of the alcohol function to the bromide derivative. Once these two intermediates are in hands, the phosphonium-phosphine ligand **1** has been obtained in 43% yield by reacting them together.

The ^{31}P-NMR spectrum shows two characteristic signals at -15.1 ppm for the phosphine moiety and at 22.7 ppm for the phosphonium group. The final gold complexes are obtained by reacting chloro(tetrahydrothiophene)gold (I) precursor with **IV** for the synthesis of **X** and bromo(tetrahydrothiophene)gold(I) precursor with **1** for the synthesis of **2**. In the latter case, we used the brominated version of the gold salt to avoid obtaining a chlorido and bromido-gold mixture induced by the bromide counter-ion of **1**. This last reaction is carried out in dichloromethane at room temperature and affords the corresponding gold(I)-phosphonium-phosphine complex **2** in 94% yield (Scheme 1). Its ^{31}P NMR spectrum shows two signals at 23.1 and 26.8 ppm.

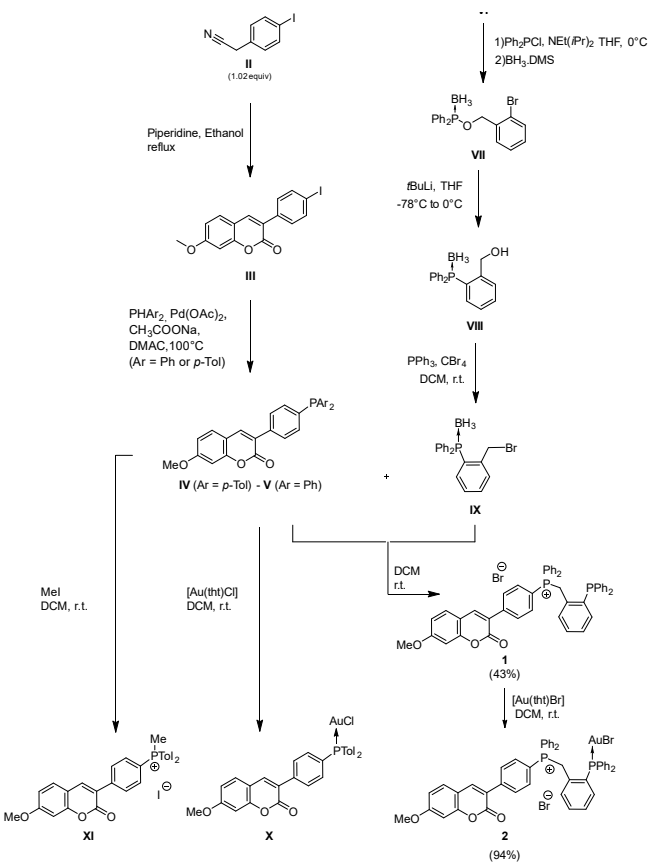

Scheme 1. Synthesis of phosphine-gold(I) complex **X**, phosphonium **XI**, and phosphonium-phosphine gold(I) complex **2**.

Photophysical properties

One of the interests of introducing a coumarin moiety, beyond its contribution from a biological activity point of view, is that it enables the tracking of the therapeutic agent by fluorescence imaging. We have therefore characterized the photophysical properties of the new gold complex **2** and its corresponding ligand **1** (Figure 2). For comparison, we have indicated the properties of **IV**, **V**, **X**, and **XI** previously measured.[49,53] It is worth noting that the maximum absorption and emission wavelengths are little affected by the various modifications: no impact of complexation with gold and bathochromic shift of 10 nm in the case of the phosphonium derivatives. Likewise, the molar absorption coefficients are similar, although they are higher for **XI**.

Conversely, quantum yields are strongly modified by the presence of a lone pair on the phosphorus. This free lone pair generates photo-induced electron transfer (PET) (e.g. ligands **IV** and **V** and **1**, even if in this last case the PET is lower, due to an increased distance between the fluorophore and the phosphorus atom). When the latter is engaged in the formation of a "P-C" bond in the case of phosphonium (e.g. **XI**) or of a "P-Au" bond for gold complexes (e.g. **X**), fluorescence is restored (**X** and **XI** 30 to 40 times brighter than **IV** respectively, and **2** is almost 70% of the brighter than **1**) (Figure 3).

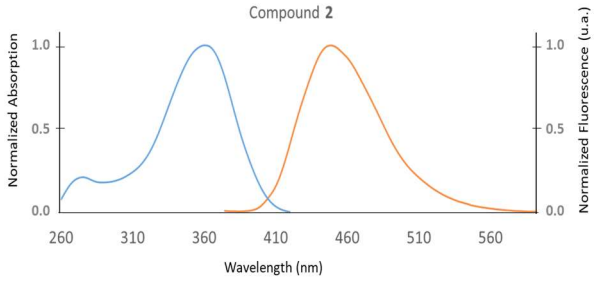

N°	λ_{abs}[a] (nm)	λ_{em}[b] (nm)	ε[c] ($M^{-1}.cm^{-1}$)	Φ_f[d] (%)
IV	348	430	25,100	3
V	348	430	25,000	5
X	350	432	25,700	83
XI	355	441	34,300	91
1	358	440	25,300	53
2	358	440	26,000	86

Figure 2. (top) normalized absorption (blue) and emission (orange) spectra of compound **2** in DMSO at 298 K. (bottom) Photophysical data of compounds **IV**, **V**, **X**, **XI**,[49] **1**, and **2** in DMSO at 298 K. [a] λ_{abs} = wavelength of maximal absorption. [b] λ_{em} = wavelength of maximal emission. [c] ε = molar absorption coefficient. [d] Φ_f = fluorescence quantum yield, reference: diphenylanthracene (Φ_f = 0.97, λ_{exc} = 355 nm, in cyclohexane[66]).

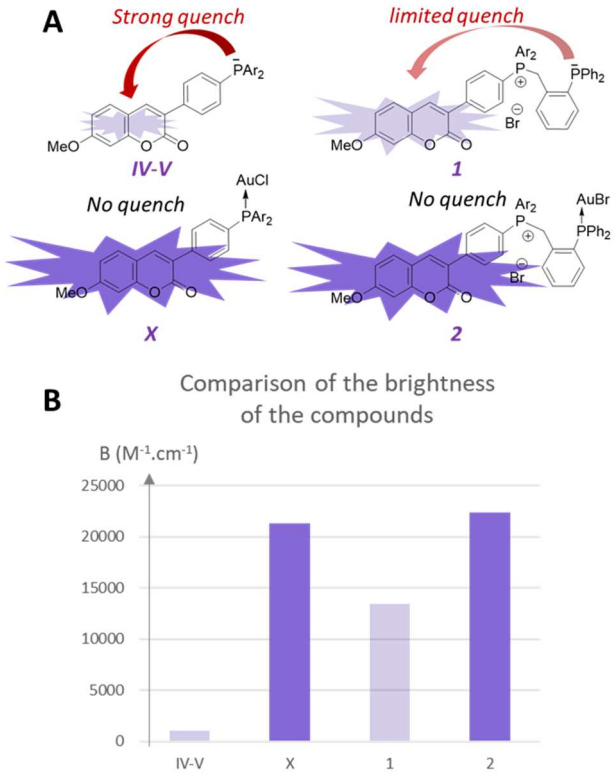

Figure 3. Explanation of the difference of quench phenomenon intensity for the different compounds (top) and its impact on the brightness (brightness, B = $\varepsilon\Phi_f$) of the corresponding compounds (bottom).

In vitro investigations

While coumarin derivatives exhibit good signal of fluorescence, their photophysical properties are not ideal for *in vitro* imaging. Indeed, their maximum absorption wavelength, which is between 350 and 360 nm is too low to be compatible with many microscopes. In addition, a low wavelength is also synonymous with high energy, thus, such excitation wavelength can degrade the tissues observed. Fortunately, we previously noticed that coumarins could respond to two-photon imaging. The advantage of this technique is that it allows the use of longer wavelength photons - in our case 700-720 nm - which will not damage the tissues.

As expected, both **X** and **2** gave good response in two-photon imaging, and thus, can be easily tracked *in vitro* (Figure 4). By looking at the images obtained by irradiation at 720 nm of CT26 cancer cells, previously incubated for 1 h at 37°C with 50 µM of the gold complex **2**, we can see that it enters the cytoplasm, even if it also appears to accumulate in vesicles. Interestingly, the power of the laser needed for obtaining an equivalent signal for **2** is three times lower than for **X**. Furthermore, no drop in fluorescence was observed during the experiments. This would tend to confirm that the "P-Au" bond is stable in a cell medium, even if in this case, we must remain cautious because the difference in brightness between **2** and its corresponding ligand **1** is by a factor of approximately 2 and not of 30 as in the case of **X** and **IV**.

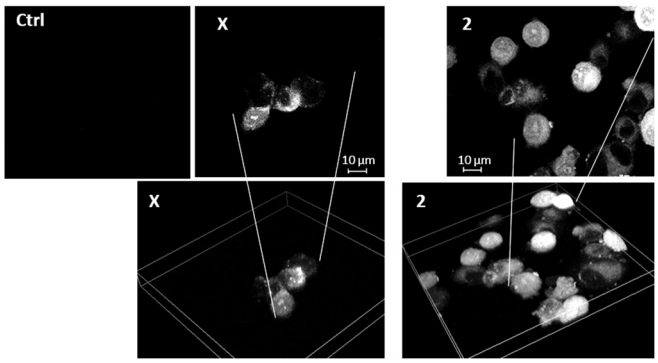

Figure 4. Biphoton images of the compounds **X** and **2** on CT26 cell line. Cells are incubated, or not (Ctrl with DMSO), with 50 µM of the compounds for 1 h at 37°C, then fixed and permeabilized with 2% paraformaldhehyde and mounted with Prolong. Two-photon images are recorded upon 720 nm excitation (Chameleon IR laser from Coherent) and fluorescence emission collected through channel 1 ("DAPI channel") 400/492 nm.

As compound **2** can be easily tracked *in vitro* by two-photon imaging, its anti-proliferative properties were evaluated on three human cell lines of lung (A549), breast (MDA-MD-231), and colon (SW480) cancers (Table 1). On the three cell lines, after 48 h, the gold complex **2** appears strongly active. It exhibits activities of the range of paclitaxel, it is 4 to 18 times more active than oxaliplatin and more than 20 times more efficient than 5-FU. Moreover, if we take the IC_{50} that we have obtained for coumarin-gold **X** on MDA-MB-231 and SW480,[49,53] **2** is 17 to 26 times more active than **X**. It appears that the modification of the structure of the complex very significantly improved its anti-proliferative activity. In addition, it would come in second position, if we compare it to the seven phosphonium-phosphine-gold (I) complexes that we had synthesized and studied previously.[61] This confirms our observations by highlighting that promoting the delocalization of the phosphonium charge over a maximum of the aromatic cycles improves the anti-proliferative properties of the compound.

Table 1. Determination of the IC_{50} values (µM) of complexes **X** and **2**, compared those of oxaliplatin and 5-FU on A549, MDA-MD-231, and SW480 cancer cell lines by crystal violet assay at 48 h (values are presented as the mean ± SEM of at least three independent experiments with three replicates).

Compound	IC_{50} (µM) A549	MDA-MB-231	SW480
X	N.T.	33.1 ± 14.8*	42.0 ± 11.7*
2	0.42 ± 0.01	1.28 ± 0.44	2.47 ± 0.97
Oxaliplatin	7.5 ± 0.40	14.4 ± 1.90	9.2 ± 1.40
5-FU	9.1 ± 0.90	22.3 ± 0.60	52.5 ± 8.40
Paclitaxel	0.33 ± 0.04	0.39 ± 0.02	2.0 ± 0.74

Before proceeding with the *in vivo* experiments, the anti-proliferative properties of **X** and **2** were investigated onto lung (LLC1), breast (4T1), and colon (CT26) murine cancer cell lines (Table 2). Indeed, given the importance of the immune system in the tumor response, we wanted to preserve it and therefore use syngeneic models. Again, complex **2** exhibits anti-proliferative properties far superior to **X**.

Table 2. Determination of the IC_{50} values (µM) of **X** and **2** compounds on LLC1, 4T1 and CT26 cancer cell lines by MTS assay at 48 h (values are presented as the mean ± SEM of at least three independent experiments with three replicates).

Compound	IC_{50} (µM)		
	LLC1	4T1	CT26
X	94.9 ± 16.0	40.2 ± 0.23	25.4 ± 0.4
2	4.81 ± 0.34	4.72 ± 0.10	4.67 ± 0.09

In vivo studies

Proliferation tests have shown that compound **2** is about as active on the three murine cancer cell lines, while **X** displays its best activity on the CT26 cancer cell line. The anti-cancer effect of **X** and **2** was therefore evaluated in Balb/c mice bearing subcutaneous CT26 tumor (Figure 5). When the tumor size reaches a volume of about 50 mm^3, the mice were injected intraperitoneally twice a week at a dose of 0.1 mg / kg of **X** or of **2**. Tumors have been measured regularly and it appears that, as might be expected, complex **X** exhibits limited anti-cancer activity at this concentration. On the other hand, phosphonium-phosphine-gold **2** has a very significant anti-cancer effect with a strong decrease of tumor growth. A similar anticancer effect was obtained by Milovanovic and coll. using a mass concentration of oxaliplatin 20 times higher than the one we used for compound **2** under conditions similar to ours.[67] Furthermore, in our case, no sign of toxicity was observed in any of the mice.

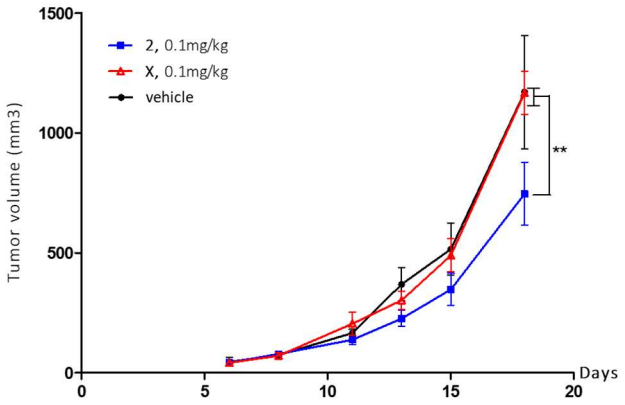

Figure 5. Anti-tumor effect of **X** and **2** compounds. CT26 Tumor-bearing BALB/c mice (n=6/group) were treated intraperitoneally twice per week with 0.1 mg/kg of compounds X or 2 (in DMSO) or with the same quantity of DMSO (vehicle). Tumor growth was determined 3 times per week using a caliper. Results are expressed as means ± SEM, Two-way Anova:*p<0.05, **p≤0.01, ***≤0.001.

Conclusion

During this study, the synthesis of a novel optical theranostic agent was described as well as its characterization. It appears that the phosphonium-phosphine unit not only increases the solubility in water but also dramatically improves the anti-proliferative properties of an average factor of 20 of the complex compared to its phosphine-gold analogue. We also noticed that it had a better signal on two-photon imaging so that it could be tracked in the cells. Finally, it exhibits very significant anti-cancer activities *in vivo* without any sign of toxicity, whilst its phosphine-gold analogue does not exhibit significant anti-cancer activity. These very promising results prompt us, in a future study, to explore in more details the mechanisms of action involved, to know whether it may be interesting to modify the ligand "X" carried by the gold to further improve the biological activity of the complex and, in parallel, to determine the maximum tolerated dose to further optimize its activity *in vivo*.

Experimental Section

Material and methods

All synthetic manipulations were carried out using standard Schlenk techniques. All reagents were purchased either from Acros Organics, Sigma-Aldrich, Fischer Scientific, Alfa Aesar, TCI or ABCR and used without further purification. THF and dichloromethane were dried over alumina cartridges using a solvent purification system MB-SPS-800 model from M. BRAUN. Column chromatography were conducted on silica gel 60-200 µm or 40-63 µm purchased from Sigma-Aldrich. NMR spectra (^{1}H, ^{13}C, ^{31}P) were recorded with Brucker 300 MHz, 500 MHz or 600 MHz apparatus, using tetramethylsilane as internal reference for ^{1}H, ^{13}C NMR, phosphoric acid (85%) as external reference for ^{31}P NMR. Abbreviations used to describe the multiplicity of the signal are: s (singlet), d (doublet), t (triplet), q (quartet), bs (broad singlet), m (multiplet). Mass spectra were performed under electrospray ionization conditions (ESI) with a Thermo LTQ Orbitrap XP. Infrared spectra were recorded on a FT-IR instrument (Bruker Alpha), and the data are given in cm^{-1}.

Synthesis

3-{4-{[(2-diphenylphosphanyl)phenyl]methyldiphenylphosphonium}phenyl}-7-methoxy-2H-chromen-2-one bromide **1** :

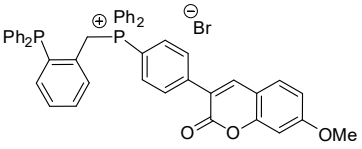

Chemical Formula: $C_{47}H_{37}BrO_3P_2$
Molecular Weight: 791.65

To a solution of [(2-bromomethyl)phenyl]diphenylphosphine borane **IX** (185 mg, 0.5 mmol) in DCM (2 mL) was added the tertiary phosphine **V** (545 mg, 1.25 mmol, 2.5 equivalents) and the reaction was stirred 24h. After removing most of the solvent, Et_2O (5 mL) was added and a precipitate appeared which was filtered and purified on silica gel using MeOH/DCM 1:10 as eluent. Compound **1** was obtained as a yellow solid in 43% yield (170 mg, 0.21 mmol).

Mp: 162°C (dec).

^{1}H NMR (500 MHz, Methylene Chloride-d_2) δ 8.19 (s, 1H, H_{aro}), 8.07 (dd, J = 8.5, 3.1 Hz, 2H, H_{aro}), 7.92 - 7.87 (m, 2H, H_{aro}), 7.71 - 7.64 (m, 5H, H_{aro}), 7.62 - 7.54 (m, 6H, H_{aro}), 7.39 - 7.23 (m, 9H, H_{aro}), 6.98 - 6.88 (m, 6H, H_{aro}), 6.88 - 6.82 (m, 1H, H_{aro}), 5.04 (d, J = 13.8 Hz, 2H, CH_2), 3.92 (s, 3H, OCH_3).

{^{1}H}^{13}C NMR (151 MHz, Methylene Chloride-d_2) δ 164.68 (C_{aro}), 160.88 (C_{aro}), 156.78 (C_{aro}), 143.72 (C_{aro}), 143.33 (d, J = 3.3 Hz, C_{aro}), 139.40 (dd, J = 12.8, 6.1 Hz, C_{aro}), 136.25 (d, J = 3.1 Hz, C_{aro}), 135.57 (d, J = 3.4 Hz, C_{aro}), 135.25 (d, J = 10.1 Hz, C_{aro}), 135.22 (d, J = 9.8 Hz, C_{aro}), 134.81 (d, J = 7.7 Hz, C_{aro}), 134.54 (d, J = 19.8 Hz, C_{aro}), 132.58 (dd, J = 24.0, 8.9 Hz, C_{aro}), 131.80 (t, J = 4.5 Hz, C_{aro}), 131.16 (d, J = 12.6 Hz, C_{aro}), 130.95 (d, J = 3.6 Hz, C_{aro}), 130.88 (C_{aro}), 130.67 (d, J = 12.8 Hz, C_{aro}), 130.50 (d, J = 3.9 Hz, C_{aro}), 130.28 (C_{aro}), 129.70 (d, J = 7.2 Hz, C_{aro}), 122.21 (C_{aro}), 118.19 (d, J = 85.8 Hz, C_{aro}), 116.93 (d, J = 87.4 Hz, C_{aro}), 113.97 (C_{aro}), 113.80 (C_{aro}), 101.24 (C_{aro}), 56.83 (OCH_3), 30.85 (dd, J = 48.3, 24.2 Hz, CH_2).

{^{1}H}^{31}P NMR (202.5 MHz, Methylene Chloride-d_2) δ 22.67 (s), -15.09 (s).

IR (cm^{-1}): 3052, 1719, 1590, 1506, 1435, 1360, 1270, 1161, 1112, 1021, 984, 939, 824, 781, 740, 718, 690, 637, 623, 595, 540, 512.

HR-MS (ESI): m/z calcd for $C_{47}H_{37}O_3P_2$ $[M-Br]^+$: 711.22124 Da; Found : 711.22307 Da.

{3-{4-{[(2-diphenylphosphanyl)phenyl]methyldiphenylphosphonium} phenyl}-7-methoxy-2H-chromen-2-one} AuBr **2** :

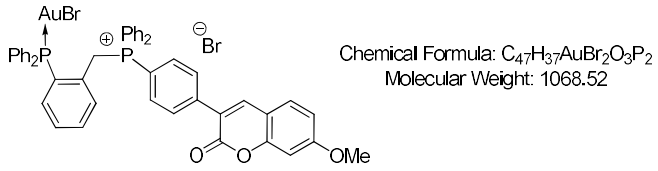

Chemical Formula: $C_{47}H_{37}AuBr_2O_3P_2$
Molecular Weight: 1068.52

To a solution of phosphine phosphonium **1** (80 mg, 0.1 mmol) in DCM (4 mL), bromo(tetrahydrothiophene) Au (I) (37 mg, 0.1 mmol) was added under argon at RT and the reaction was stirred for 1h. The resulting mixture was concentrated and the product was precipitated using pentane and washed twice with a mixture of pentane/DCM 10:1. Complex **2** was obtained as a white solid in 94% yield (100 mg, 0.094 mmol).

Mp : 188 °C (dec).

^{1}H NMR (500 MHz, Chloroform-*d*) δ 8.26 (s, 1H, H_{aro}), 8.11 (d, *J* = 7.1 Hz, 2H, H_{aro}), 7.85-7.78 (m, 2H, H_{aro}), 7.72 - 7.60 (m, 11H, H_{aro}), 7.60 - 7.43 (m, 8H, H_{aro}), 7.43-7.34 (m, 5H, H_{aro}), 6.93 (dd, *J* = 8.6, 2.4 Hz, 1H, H_{aro}), 6.87 (d, *J* = 2.4 Hz, 1H, H_{aro}), 6.80 (dd, *J* = 12.6, 7.8 Hz, 1H, H_{aro}), 5.66 (d, *J* = 14.9 Hz, 2H, CH_2), 3.92 (s, 3H, OCH_3).

{^{1}H}^{13}C NMR (151 MHz, Methylene Chloride-d_2) δ 164.64 (C_{aro}), 160.86 (C_{aro}), 156.76 (C_{aro}), 143.80 (C_{aro}), 143.45 (d, *J* = 3.3 Hz, C_{aro}), 136.48 (d, *J* = 3.2 Hz, C_{aro}), 136.26 (d, *J* = 7.5 Hz, C_{aro}), 135.48 (d, *J* = 11.2 Hz, C_{aro}), 135.47 (d, *J* = 10.1 Hz, C_{aro}), 135.26 (d, *J* = 14.3 Hz, C_{aro}), 133.6 (C_{aro}), 133.56 (d, *J* = 2.3 Hz, C_{aro}), 133.27 (m, C_{aro}), 132.68 (dd, *J* = 10.6, 7.7 Hz, C_{aro}), 132.51 (d, *J* = 9.7 Hz, C_{aro}), 131.46 (d, *J* = 12.7 Hz, C_{aro}), 131.04 (d, *J* = 12.9 Hz, C_{aro}), 130.85 (C_{aro}), 130.70 (d, *J* = 12.2 Hz, C_{aro}), 129.82 (dd, *J* = 57.5, 6.7 Hz, C_{aro}), 127.87 (d, *J* = 62.9 Hz, C_{aro}), 122.31 (C_{aro}), 117.70 (d, *J* = 86.4 Hz, C_{aro}), 116.43 (d, *J* = 87.4 Hz, C_{aro}), 113.94 (C_{aro}), 113.82 (C_{aro}), 101.24 (C_{aro}), 56.82 (OCH_3), 30.36 (dd, *J* = 50.1, 12.8 Hz, CH_2).

{^{1}H}^{31}P NMR (202.5 MHz, Chloroform-*d*) δ 26.76 (s), 23.12 (s).

IR (cm^{-1}): 2926, 1719, 1589, 1506, 1435, 1403, 1360, 1270, 1216, 1161, 1100, 1024, 996, 939, 822, 774, 748, 717, 688, 622, 596, 543, 495.

HR-MS (ESI): m/z calcd for $C_{47}H_{37}AuBrO_3P_2$ $[M-Br]^+$: 987.10613 Da; Found: 987.10788 Da.

Cell lines and culture conditions:

Human colon cancer (SW 480), breast cancer (MDA-MB-231), and lung cancer (A-549) and murine colon cancer (CT26), breast cancer (4T1), and lung cancer (LLC1)cell lines were obtained from the American Type Culture Collections (Manassas, VA, United States). They were cultured in RPMI 1640 (SW480, MDA-MB-231, A-549 and CT26) or DMEM (4T1 and LLC1) medium (Biowhittaker, France) supplemented with 10% fetal bovine serum (Biowhittaker, France) at 37°C under a humidified atmosphere containing 5% CO_2. All cell lines were maintained as exponentially growing monolayers in mycoplasma free culture condition checked by polymerase chain reaction (PCR) analysis (PCR Mycoplasma Test Kit I/C, PromoKine, PromoCell France).

Drug solutions:

The newly phosphonium-phosphine gold(I) complex **2** was diluted into dimethylsulfoxide (DMSO) (Sigma, France). Reference molecules, approved in clinic for colon, breast or lung cancer, were acquired from commercial solutions: oxaliplatin (Oxaliplatin Dakota Pharm® 5 mg/ml), 5-fluorouracil (Fluorouracil Accord® 50 mg/ml) and paclitaxel (Paclitaxel Kabi® 6 mg/ml). In cell culture, maximum concentration of DMSO did not exceed 3 % in the medium.

Determination of cytotoxicity:

The crystal violet staining test and MTS assay were chosen to determine the cytotoxicity of different compounds on respectively human and murine cancer cell lines. 10^5 cells were seeded in 96-well plates and incubated for 24h to allow for cell adherence. Twenty four hours later, cells were treated for 48 hours by increasing concentrations (from 0 to 500 µM or from 0 to 25 µM according to the drug) of the newly synthetized or reference molecules. After treatment, cytotoxicity on human cancer cell lines was assessed by crystal violet staining, at λ = 570 nm (spectrophotometer UVM 340, Bioserv). The cytotoxic activity of compounds and drug references on murine cancer cell lines was determined using the MTS assay (Promega®). Thereafter, 20 µL of MTS (3-(4,5-dimethylthiazol-2-yl)-5-(3-carboxymethoxy phenyl)-2-(4-sulfophenyl)-2H-tetrazolium, Promega, Charbonnières, France) was added in each well and absorbance at 490 nm was measured after 3h incubation at 37 °C. The resulting IC50 values were calculated using GraphPad Prism 5.0 software. Each treatment was performed in three independent experiments.

Determination of the anti-tumor effect:

All experiments followed the guidelines of the Federation of European Animal Science Associations and were all approved by the Ministry of agriculture and food (France, Apafis number: #15181) and by the Ethics Committee of Burgundy University (Dijon, France).
In order to test the potential anti-tumor effect of **2** and **X** compounds, Balb/c mice (8 weeks old, Charles River, France) were grafted by subcutaneous injection of murine colon cancer CT26 cells (5.10^5 cells). Seven days after tumor implantation (tumor volume around 50 mm^3), tumor-bearing mice were randomized into three groups, one received 0.1 mg/kg of **2** or **X** compounds (in DMSO) and the other received the same quantity of DMSO in saline (vehicle) by intraperitoneal injection (IP). These IP injections were performed two times a week and tumor volume assessed three times per week. Mice whose tumor reached 1,500 mm^3 were euthanized due to ethical reasons.

Acknowledgements

The Ministère de l'Enseignement Supérieur et de la Recherche, the Centre National de la Recherche Scientifique (CNRS), the Conseil Régional de Bourgogne (PhD JCE grant # 2018Y-08158), and the French Research National Agency (ANR) *via* project JCJC ''SPID" ANR-16-CE07-0020 are gratefully acknowledged. This work is part of the projects ''Pharmacoimagerie et agents théranostiques" et ''Chimie durable, environnement et agroalimentaire" supported by the Université de Bourgogne and the Conseil Régional de Bourgogne through the Plan d'Actions Régional pour l'Innovation (PARI) and the European Union through the PO FEDER-FSE Bourgogne 2014/2020 programs. We thank the Conseil Régional de Bourgogne Franche-Comté for its support via the project ANER "AZTHEC". This work was also supported by grants from Ligue contre le Cancer, Comité de Côte d'Or. FrenchBIC, and GDR AIM are acknowledged for fruitful discussion. Ms M.-J. Penouilh and Mr. Q. Bonnin are gratefully acknowledged for HR-MS analysis, and Dr M. Picquet for NMR analyses. The authors would like to thank Dr V. Comte-Candas, Ms. P. Girard, and Ms. M. Guillemin for their technical support, Ms. V. Saint-Giorgio (zootechny center, UBFC), Ms. A. Legrand (Cytometry Plateform, UMR1231 UBFC), and Ms. E. Noirot (Plateforme DImaCell, AgroSup Dijon INRAE, Université Bourgogne Franche-Comté).

Keywords: theranostic • gold complex • fluorescence • coumarin • phosphine

References:

[1] B. Rosenberg, L. Van Camp, T. Krigas, *Nature* **1965**, *205*, 698–699.
[2] B. Rosenberg, L. Vancamp, J. E. Trosko, V. H. Mansour, *Nature* **1969**, *222*, 385–386.
[3] S. Dasari, P. Bernard Tchounwou, *Eur. J. Pharmacol.* **2014**, *740*, 364–378.
[4] J. Reedijk, *Eur. J. Inorg. Chem.* **2009**, *2009*, 1303–1312.
[5] L. Kelland, *Nat. Rev. Cancer* **2007**, *7*, 573–584.

[6] M. Cini, T. D. Bradshaw, S. Woodward, *Chem. Soc. Rev.* **2017**, *46*, 1040–1051.
[7] E. Alessio, *Eur. J. Inorg. Chem.* **2017**, *2017*, 1549–1560.
[8] C. Gaiddon, I. Gross, X. Meng, M. Sidhoum, G. Mellitzer, B. Romain, J.-B. Delhorme, A. Venkatasamy, A. C. Jung, M. Pfeffer, *Molecules* **2021**, *26*, 5386.
[9] Y. Zhao, Y. Kang, F. Xu, W. Zheng, Q. Luo, Y. Zhang, F. Jia, F. Wang, in *Advances in Inorganic Chemistry* (Eds.: P.J. Sadler, R. van Eldik), Academic Press, **2020**, pp. 257–285.
[10] K.-C. Tong, D. Hu, P.-K. Wan, C.-N. Lok, C.-M. Che, in *Advances in Inorganic Chemistry* (Eds.: P.J. Sadler, R. van Eldik), Academic Press, **2020**, pp. 87–119.
[11] B. S. Murray, P. J. Dyson, *Curr. Opin. Chem. Biol.* **2020**, *56*, 28–34.
[12] M. Miller, A. Mellul, M. Braun, D. Sherill-Rofe, E. Cohen, Z. Shpilt, I. Unterman, O. Braitbard, J. Hochman, E. Y. Tshuva, Y. Tabach, *iScience* **2020**, *23*, DOI 10.1016/j.isci.2020.101262.
[13] L. Habala, J. Valentová, *Ceska Slov Farm* **2020**, *69*, 3–16.
[14] J. Ceramella, A. Mariconda, D. Iacopetta, C. Saturnino, A. Barbarossa, A. Caruso, C. Rosano, M. S. Sinicropi, P. Longo, *Bioorg. Med. Chem. Lett.* **2020**, *30*, 126905.
[15] M. Bouché, C. Hognon, S. Grandemange, A. Monari, P. C. Gros, *Dalton Trans.* **2020**, *49*, 11451–11466.
[16] S. K. Nandanwar, H. J. Kim, *ChemistrySelect* **2019**, *4*, 1706–1721.
[17] G. Gupta, P. Kumari, J. Y. Ryu, J. Lee, S. M. Mobin, C. Y. Lee, *Inorg. Chem.* **2019**, *58*, 8587–8595.
[18] S. Tasan, O. Zava, B. Bertrand, C. Bernhard, C. Goze, M. Picquet, P. L. Gendre, P. Harvey, F. Denat, A. Casini, E. Bodio, *Dalton Trans.* **2013**, *42*, 6102–6109.
[19] F. Chotard, L. Dondaine, C. Balan, A. Bettaïeb, C. Paul, P. L. Gendre, E. Bodio, *New J. Chem.* **2018**, *42*, 8105-8112.
[20] O. Florès, A. Trommenschlager, S. Amor, F. Marques, F. Silva, L. Gano, F. Denat, M. P. C. Campello, C. Goze, E. Bodio, P. L. Gendre, *Dalton Trans.* **2017**, *46*, 14548–14555.
[21] R. Lescure, M. Privat, J. Pliquett, A. Massot, O. Baffroy, B. Busser, P.-S. Bellaye, B. Collin, F. Denat, A. Bettaïeb, L. Sancey, C. Paul, C. Goze, E. Bodio, *Eur. J. Med. Chem.* **2021**, 113483.
[22] S. Spreckelmeyer, M. van der Zee, B. Bertrand, E. Bodio, S. Stürup, A. Casini, *Front. Chem.* **2018**, *6*, DOI 10.3389/fchem.2018.00377.
[23] A. Trommenschlager, F. Chotard, B. Bertrand, S. Amor, L. Dondaine, M. Picquet, P. Richard, A. Bettaeib, P. Le Gendre, C. Paul, C. Goze, E. Bodio, *Dalton Trans.* **2017**, *46*, 8051-8056.
[24] M. Wenzel, A. de Almeida, E. Bigaeva, P. Kavanagh, M. Picquet, P. Le Gendre, E. Bodio, A. Casini, *Inorg. Chem.* **2016**, *55*, 2544–2557.
[25] T. G. Benedek, *J Hist Med Allied Sci* **2004**, *59*, 50–89.
[26] H. Scheffler, Y. You, I. Ott, *Polyhedron* **2010**, *29*, 66–69.
[27] S. Medici, M. Peana, V. M. Nurchi, J. I. Lachowicz, G. Crisponi, M. A. Zoroddu, *Coord. Chem. Rev.* **2015**, *284*, 329–350.
[28] S. P. Pricker, *Gold Bull* **1996**, *29*, 53–60.
[29] I. Ott, *Coord. Chem. Rev.* **2009**, *253*, 1670–1681.
[30] S. J. Berners-Price, A. Filipovska, *Metallomics* **2011**, *3*, 863–873.
[31] B. Bertrand, A. Casini, *Dalton Trans* **2014**, *43*, 4209–4219.
[32] O. Florès, D. Velic, N. Mabrouk, A. Bettaïeb, C. Tomasoni, J.-M. Robert, C. Paul, C. Goze, C. Roussakis, E. Bodio, *ChemBioChem* **2019**, *20*, 2255–2261.
[33] C. K. Mirabell, R. K. Johnson, D. T. Hill, L. F. Faucette, G. R. Girard, G. Y. Kuo, C. M. Sung, S. T. Crooke, *J. Med. Chem.* **1986**, *29*, 218–223.
[34] T. Marzo, L. Massai, A. Pratesi, M. Stefanini, D. Cirri, F. Magherini, M. Becatti, I. Landini, S. Nobili, E. Mini, O. Crociani, A. Arcangeli, S. Pillozzi, T. Gamberi, L. Messori, *ACS Med. Chem. Lett.* **2019**, *10*, 656–660.
[35] F. H. Abdalbari, C. M. Telleria, *Discov Onc* **2021**, *12*, 42.
[36] X. Zhang, K. Selvaraju, A. A. Saei, P. D'Arcy, R. A. Zubarev, E. SJ. Arnér, S. Linder, *Biochimie* **2019**, *162*, 46–54.
[37] E. V. Capparelli, R. Bricker-Ford, M. J. Rogers, J. H. McKerrow, S. L. Reed, *Antimicrob. Agents Ch.* **2017**, *61*, DOI 10.1128/AAC.01947-16.
[38] L. R. A. James, Z.-Q. Xu, R. Sluyter, E. L. Hawksworth, C. Kelso, B. Lai, D. J. Paterson, M. D. de Jonge, N. E. Dixon, J. L. Beck, S. F. Ralph, C. T. Dillon, *J. Inorg. Biochem.* **2015**, *142*, 28–38.
[39] T. Onodera, I. Momose, M. Kawada, *Chem. Pharm. Bull.* **2019**, *67*, 186–191.
[40] T. M. Simon, D. H. Kunishima, G. J. Vibert, A. Lorber, *Cancer Res.* **1981**, *41*, 94–97.
[41] B. Bertrand, G. M. Groothuis, A. Casini, L. Stefan, E. Bodio, P. Richard, P. Le Gendre, D. Monchaud, M. Picquet, *J. Biol. Inorg. Chem.* **2014**, *19*, S589–S589.
[42] B. Bertrand, A. de Almeida, E. P. M. van der Burgt, M. Picquet, A. Citta, A. Folda, M. P. Rigobello, P. Le Gendre, E. Bodio, A. Casini, *Eur. J. Inorg. Chem.* **2014**, 4532-4536.
[43] B. Bertrand, L. Stefan, M. Pirrotta, D. Monchaud, E. Bodio, P. Richard, P. Le Gendre, E. Warmerdam, M. H. de Jager, G. M. M. Groothuis, M. Picquet, A. Casini, *Inorg. Chem.* **2014**, *53*, 2296–2303.
[44] M. Wenzel, E. Bigaeva, P. Richard, P. Le Gendre, M. Picquet, A. Casini, E. Bodio, *J. Inorg. Biochem.* **2014**, *141*, 10–16.
[45] B. Bertrand, E. Bodio, P. Richard, M. Picquet, P. Le Gendre, A. Casini, *J. Organomet. Chem.* **2015**, *775*, 124–129.
[46] B. Bertrand, A. Citta, I. L. Franken, M. Picquet, A. Folda, V. Scalcon, M. P. Rigobello, P. L. Gendre, A. Casini, E. Bodio, *J Biol Inorg Chem* **2015**, *20*, 1005–1020.
[47] B. Bertrand, A. de Almeida, E. P. M. van der Burgt, A. Citta, A. Folda, E. Bodio, M. Picquet, M. P. Rigobello, P. Le Gendre, A. Casini, *J. Biol. Inorg. Chem.* **2014**, *19*, S792–S792.
[48] P.-E. Doulain, S. Tasan, R. Decreau, C. Paul, P. Le Gendre, F. Denat, C. Goze, E. Bodio, *J. Biol. Inorg. Chem.* **2014**, *19*, S793–S793.
[49] M. Ali, L. Dondaine, A. Adolle, C. Sampaio, F. Chotard, P. Richard, F. Denat, A. Bettaieb, P. Le Gendre, V. Laurens, C. Goze, C. Paul, E. Bodio, *J. Med. Chem.* **2015**, *58*, 4521–4528.
[50] P.-E. Doulain, R. Decréau, C. Racoeur, V. Goncalves, L. Dubrez, A. Bettaieb, P. L. Gendre, F. Denat, C. Paul, C. Goze, E. Bodio, *Dalton Trans.* **2015**, *44*, 4874–4883.
[51] B. Bertrand, P.-E. Doulain, C. Goze, E. Bodio, *Dalton Trans.* **2016**, *45*, 13005–13011.
[52] J. Pliquett, S. Amor, M. Ponce-Vargas, M. Laly, C. Racoeur, Y. Rousselin, F. Denat, A. Bettaeib, P. Fleurat-Lessard, C. Paul, C. Goze, E. Bodio, *Dalton Trans.* **2018**, *47*, 11203-11218.
[53] L. Dondaine, D. Escudero, M. Ali, P. Richard, F. Denat, A. Bettaieb, P. Le Gendre, C. Paul, D. Jacquemin, C. Goze, E. Bodio, *Eur. J. Inorg. Chem.* **2016**, 545–553.
[54] J. M. Madar, L. A. Shastri, S. L. Shastri, M. Holiyachi, N. Naik, R. Kulkarni, F. Shaikh, V. Sungar, *Synthetic Commun.* **2018**, *48*, 375–386.
[55] M. Holiyachi, S. Samundeeswari, B. M. Chougala, N. S. Naik, J. Madar, L. A. Shastri, S. D. Joshi, S. R. Dixit, S. Dodamani, S. Jalalpure, V. A. Sunagar, *Monatsh Chem* **2018**, 1–15.
[56] A. Samala, K. G, S. K. Bagh, *Der Pharma Chemica* **2016**, *8*, 19–24.
[57] Y. A. Selim, N. H. Ouf, *Org. Med. Chem. Lett.* **2012**, *2*, 1.
[58] A. Trommenschlager, F. Chotard, B. Bertrand, S. Amor, P. Richard, A. Bettaïeb, C. Paul, J.-L. Connat, P. Le Gendre, E. Bodio, *ChemMedChem* **2018**, *13*, 2408–2414.
[59] T. Guina, F. Biasi, S. Calfapietra, M. Nano, G. Poli, *Ann. N. Y. Acad. Sci.* **2015**, *1340*, 95–103.
[60] D. Lionel, L. Christophe, A. Marc, C. Jean-Luc, *Ther Clin Risk Manag* **2006**, *2*, 159–168.
[61] B. Rousselle, F. Bouyer, J. Bayardon, M. Laly, F. Ghiringhelli, Y. Rousselin, E. Bodio, R. Malacea-Kabbara, *Dalton Trans.* **2021**, *50*, 4880–4889.
[62] M. P. Murphy, *Biochimica et Biophysica Acta (BBA) - Bioenergetics* **2008**, *1777*, 1028–1031.
[63] M. Millard, D. Pathania, Y. Shabaik, L. Taheri, J. Deng, N. Neamati, *PLoS ONE* **2010**, *5*, e13131.
[64] S. Jayakumar, R. S. Patwardhan, D. Pal, B. Singh, D. Sharma, V. K. Kutala, S. K. Sandur, *Free Radical Bio. Med.* **2017**, *113*, 530–538.
[65] J. J. Hanthorn, E. Haidasz, P. Gebhardt, D. A. Pratt, *Chem. Commun.* **2012**, *48*, 10141–10143.
[66] A. M. Brouwer, *Pure Appl. Chem.* **2011**, *83*, 2213–2228.
[67] M. Savic, A. Arsenijevic, J. Milovanovic, B. Stojanovic, V. Stankovic, A. Rilak Simovic, D. Lazic, N. Arsenijevic, M. Milovanovic, *Molecules* **2020**, *25*, 4699.

Entry for the Table of Contents

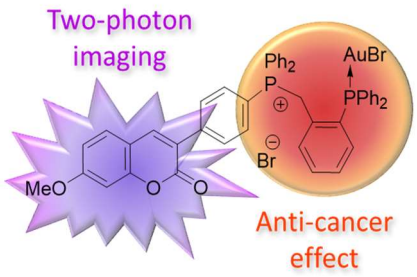

A promising gold-based optical theranostic agent was conceived. This phosphine-phosphonium gold(I) complex can be tracked by two-photon imaging thanks to a coumarin moiety. It displayed strong anti-proliferative properties against cancer cell lines and induced an anti-cancer effect *in vivo*.

Institute and/or researcher Twitter usernames: ((optional))

@ICMUB